

Ag^{2+} . Two other signals do not represent silver species: a singlet A with $g = 2.003$ is due to centers induced radiolytically in the silicoaluminum framework and a doublet of narrow H lines ($A_{\text{iso}} = 50.7$ mT, $g_{\text{iso}} = 2.002$) derives from hydrogen atoms. At 170 K signals A and H decay and then the Ag_8^{n+} multiplet is recorded practically without any interference from other signals. Owing to that it is possible to compare the experimental and simulated spectra of Ag_8^{n+} . The dashed line in Fig.2 shows that the shape and line intensity ratios in both spectra are similar provided that our assignment of the EPR nonet to octamer silver clusters is correct. At higher temperatures, Ag_8^{n+} signal decays quickly and it is barely recorded at 200 K.

Till now, the biggest radiation-induced silver cluster identified in molecular sieves was silver hexamer located in sodalite cage of zeolite A. A silver octamer Ag_8^{n+} was previously reported in hydrogen reduced Ag-A zeolite, but its spin Hamiltonian parameters ($A_{\text{iso}} = 5.2$ mT, $g = 2.025$, [5]) were completely different than the parameters of silver octamer stabilized in sodalite crystals. Especially the difference between g values is significant. All Ag_n^{n-1} clusters have g values in the range 1.970-2.000 considerably smaller than the g value of the free electron that equals 2.0023. Based on g value we tentatively assign a nine-line multiplet to Ag_8^{7+} clusters. Then silver octamer reported earlier [5] would have a different charge.

The fact that the multiplet spectrum of Ag_8^{7+} is observed directly after irradiation at 77 K univocally proves that silver agglomeration proceeds according to the second pathway described above. During sodalite dehydration Ag^+ cations migrate and agglomerate in such a way that some cages are loaded with 8 Ag^+ leaving the others empty. Such arrangements of close cations constitute the perfect trapping sites for electrons generated during low temperature radiolysis. The studies of electron

traps in frozen solutions proved that the traps can be rearranged structurally even at low temperature in order to minimize the energy of the system. The rearrangement of Ag^+ around trapped electron should change the spin density on silver nuclei and observed hyperfine splittings. In the temperature range 110-170 K we did not record any changes in the value of silver hyperfine splitting. This prompts us to assume that preexisting traps of eight Ag^+ cations do not rearrange after electron trapping or the structural changes proceed rapidly at 77 K.

Earlier, in gamma-irradiated polycrystalline Ag-SOD, we observed an EPR multiplet with similar hyperfine splitting ($A_{\text{iso}} = 8.2$ mT) which was assigned to Ag_6^{5+} hexamer [6]. In those samples, additionally to the multiplet the doublet of Ag^0 atoms was recorded all over temperature range. The present results indicate that other interpretation of EPR multiplet in polycrystalline samples is possible. Because Ag^0 doublet could overlap with the weak outer lines of EPR nonet ($hfs = 8.3$ mT), Ag_8^{7+} cluster might be also stabilized in polycrystalline Ag-SOD samples. The additional studies will be undertaken to prove that hypothesis.

References

- [1]. Michalik J., Sadlo J., Yu J.-S., Kevan L.: *Colloids Surf. A*, **115**, 239-247 (1996).
- [2]. Morton J.R., Preston K.F.: *J. Magn. Reson.*, **68**, 121-128 (1986).
- [3]. Sadlo J.: *Paramagnetic Silver Clusters in Molecular Sieves*. Ph.D. Thesis, 2000 (in Polish).
- [4]. Bye K.L., White E.A.D.: *J. Cryst. Growth*, **6**, 355-356 (1970).
- [5]. Grobet P.J., Schoonheydt R.A.: *Surf. Sci.*, **156**, 893-898 (1985).
- [6]. Michalik J., Sadlo J., Danilczuk M., Perlinska J., Yamada H.: *Stud. Surf. Sci. Catal.*, **142**, 311-318 (2002).

SOME SUBSTITUTED THIOETHERS ARE ABLE TO SPONTANEOUSLY REDUCE Cu^{II} IMIDAZOLE COMPLEXES.

A POSSIBLE IMPLICATION FOR THE COPPER-RELATED NEUROTOXIC PROPERTIES OF ALZHEIMER'S AMYLOID β -PEPTIDE

Katarzyna Serdiuk^{1/}, Jarosław Sadło, Małgorzata Nyga, Dariusz Pogocki

^{1/} Pedagogical University of Częstochowa, Poland

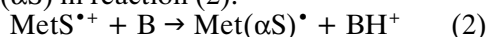
The amyloid β -peptide (βA) dependence formation of free radicals and reactive oxygen species has been identified as an important pathway of Alzheimer's disease pathology. To some extent neurotoxicity of βA seems to correlate with its ability to both formation of free radicals and spontaneous reduction of complexed copper, whose concentration in the amyloid plaques reaches 400 μM [1].

The involvement of Met^{35} in copper reduction by βA is an important, although not completely understood, phenomenon. It has been postulated that N-terminally bonded Cu^{II} is reduced by the electron originating from the C-terminal methionine

(Met) residue [2-4]. However, the direct oxidation of thioether sulfur of Met^{35} by copper appears unfavorable based on the reduction potentials of the $\beta\text{A}(\text{Cu}^{\text{I}}/\text{Cu}^{\text{II}})$ and $\text{MetS}^{*+}/\text{Met}$ couples. In normal conditions the difference between the reduction potentials of $\beta\text{A}(\text{Cu}^{\text{I}}/\text{Cu}^{\text{II}})$ (0.5-0.55 V vs. Ag/AgCl) [4] and $\text{MetS}^{*+}/\text{Met}$ (1.26-1.5 V vs. Ag/AgCl) [5-8], is about ~ 0.7 -1.0 V, thus equilibrium (1) should be shifted to far left-hand side [9].

$\text{MetS} + \beta\text{A}(\text{Cu}^{\text{II}}) \rightleftharpoons \beta\text{A}(\text{Cu}^{\text{I}}) + \text{MetS}^{*+}$ (1)
However, products of reaction can be efficiently removed from equilibrium (1), which can be, therefore, dragged to the right-hand side. One of poss-

ible mechanisms of removing MetS^{*+} from the equilibrium is the formation of α -(alkylthio)alkyl radicals (αS) in reaction (2):



Therefore, in this work we studied spontaneous reactions leading to α -(alkylthio)alkyl radicals, which may influence equilibrium (1), accelerating oxidation of the Met residue in peptides.

We designed a system, in which complexes of Cu^{II} with imidazole (Im) mimic cupric site of βA . The fifth fold excess of imidazole over Cu^{2+} guarantee that at least 95% of copper is complexed as $\text{Cu}(\text{Im})_4^{2+}$ -type complex, whose spectral and redox characteristic is well known ($\lambda_{\text{max}} \approx 590 \text{ nm}$ ($\epsilon = 53 \pm 2 \text{ M}^{-1}\text{cm}^{-1}$) [10] and $E^0(\text{Cu}^{\text{II}}/\text{Cu}^{\text{I}}) \leq 0.2 \text{ V}$ and $E^0(\text{Cu}^{\text{I}}/\text{Cu}^0) \leq 0.6 \text{ V vs. SCE}$ – saturated calomel electrode) [11]. On the other hand, the Met residue was mimicked by organic thioethers (I-IV) substituted in the α position. Such substitution should significantly influence the rate of formation α -(alkylthio)alkyl radicals in the reactions of deprotonation and decarboxylation, and therefore in some cases facilitate the reduction of $\text{Cu}(\text{Im})_4^{2+}$.

(I) $\text{HO}_2\text{CCH}_2\text{SCH}_2\text{CO}_2\text{H}$

(II) $\text{HO}_2\text{CCH}_2\text{CH}_2\text{SCH}_2\text{CH}_2\text{CO}_2\text{H}$

(III) $\text{CH}_3\text{SCH}_2\text{CO}_2\text{H}$

(IV) $\text{CH}_3\text{SCH}_2\text{CO}_2\text{NH}_2$

The reduction of $\text{Cu}(\text{Im})_4^{2+}$ by thioethers was investigated in an air or argon saturated aqueous solution containing $1.5 \times 10^{-2} \text{ M CuCl}_2$, $(4.5\text{-}7.5) \times 10^{-2} \text{ M Im}$, and $(0.32\text{-}1.5) \times 10^{-2} \text{ M}$ of thioethers at pH 5.87-6.04, incubated at 37 and 50°C. For all thioethers we monitored the decay of the UV-VIS absorption and the electron spin resonance (ESR) signal of paramagnetic Cu^{II} . For the compounds I-III the yield of decarboxylation was measured applying head-space gas-chromatography.

In the argon saturated samples containing thioethers I and III efficient decarboxylation was observed (Fig.1). Whereas in the air saturated solution the yield of CO_2 was decreased by ca. 30% compare to argon saturated solutions. For thioether II, the yield of decarboxylation was negligible in both air and argon saturated solutions. The oxida-

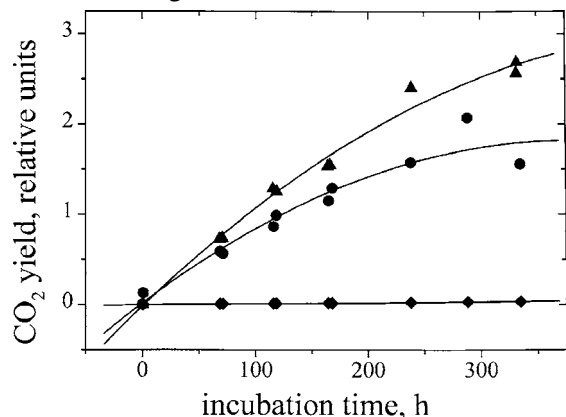


Fig.1. The yield of CO_2 as a function of the incubation time at 50°C in aqueous solutions containing $0.75 \times 10^{-2} \text{ M}$ thioether, $1.5 \times 10^{-2} \text{ M CuCl}_2$ and $7.5 \times 10^{-2} \text{ M Im}$: triangle – thioether I in argon saturated solution, circle – thioether I in air saturated solution, diamond – thioether III in argon saturated solution.

tion of thioethers I and III in the argon saturated solutions was accompanied by precipitation of copper mirror on the surface of the reactor, visible after ca. 300 h of incubation at 50°C. Simultaneously, during the incubation of $\text{Cu}(\text{Im})_4^{2+}$ with thioethers I, III and IV we observed the decay of the ESR signal (Fig.2) together with the decay of the UV-VIS absorption of $\text{Cu}(\text{Im})_4^{2+}$. In all cases

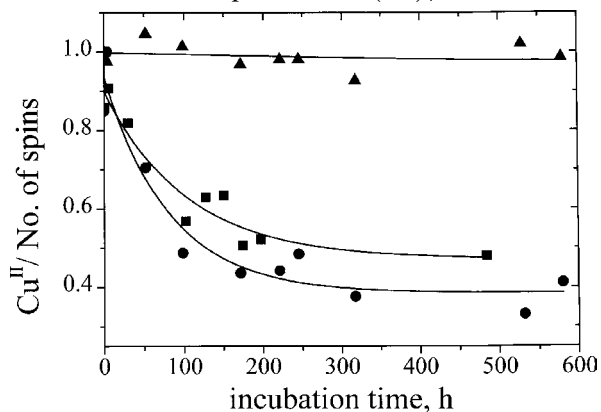
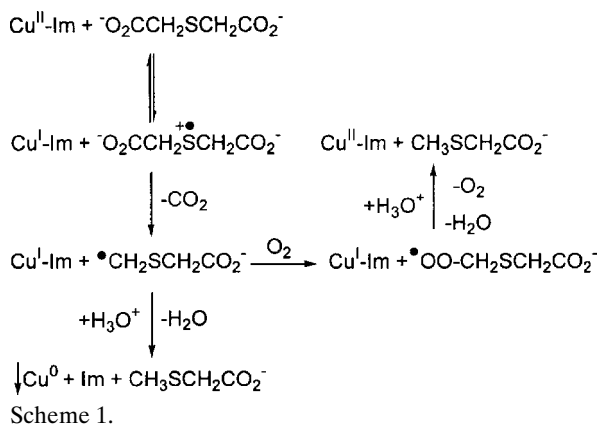


Fig.2. The ESR signal changes (represented as number of spins Cu^{II}) vs. incubation time at 50°C in argon saturated solutions containing the thioethers: square – thioether I $0.75 \times 10^{-2} \text{ M}$, CuCl_2 $1.5 \times 10^{-2} \text{ M}$, Im $4.5 \times 10^{-2} \text{ M}$; circle – thioether IV $0.75 \times 10^{-2} \text{ M}$, CuCl_2 $1.5 \times 10^{-2} \text{ M}$, Im $4.5 \times 10^{-2} \text{ M}$; triangle – CuCl_2 $1.5 \times 10^{-2} \text{ M}$, Im $4.5 \times 10^{-2} \text{ M}$.

where decay of $\text{Cu}(\text{Im})_4^{2+}$ is observed (thioethers I, III, IV), the density functional theory (DFT) calculations show that decarboxylation or deprotonation of thioether sulfide radical-cation leads to the formation of resonance stabilized radicals ($E_s \approx 10 \text{ kcal/mol}$ for III^{\bullet} and $E_s \approx 19 \text{ kcal/mol}$ for IV^{\bullet}). Whereas, for thioether III, where one may expect decarboxylation leading to the formation of alkyl radicals ($E_s \approx 0$), neither decarboxylation nor $\text{Cu}(\text{Im})_4^{2+}$ reduction was observed.

The significant differences observed in the yield of $\text{Cu}(\text{Im})_4^{2+}$ reduction between air and argon saturated solutions, and the lack of metallic copper precipitation in the presence of oxygen, suggest that oxygen takes part in the process. The presence of oxygen in solution can be a reason of partial reversibility of copper reduction.

The mechanism shown in Scheme 1 is a preliminary attempt to rationalize current observation for thioether I. This requires, however, additional experimental support.



The α -carboxylate substituted thioethers are able to spontaneously reduce $\text{Cu}(\text{Im})_4^{2+}$, since the process is "driven" by irreversible decarboxylation of S-centered radical-cation. Release of CO_2 is accompanied by an increase of entropy and thus is thermodynamically favored. Similarly, α -amide substituted thioethers can reduce $\text{Cu}(\text{Im})_4^{2+}$, taking advantage of stabilization of arising α -(alkylthio)alkyl radicals by the captodative effect.

The future of this project is to design a system, in which the influence of factors like the proton acceptors concentration, ionic strength, molecular oxygen concentration, and pH on the reduction of cupric complexes by thioethers can be investigated as these factors vary upon the oxidative stress and inflammation accompanying Alzheimer's disease.

References

- [1]. Pogocki D.: Acta Neurobiol. Exp., 63, 131-145 (2003) with all references cited therein.
- [2]. Varadarajan S., Kanski J., Aksenova M., Lauderback C., Butterfield D.A.: J. Am. Chem. Soc., 123, 5625-5631 (2001).
- [3]. Rauk A., Armstrong D.A., Fairlie D.P.: J. Am. Chem. Soc., 122, 9761-9767 (2000).
- [4]. Huang X. *et al.*: J. Biol. Chem., 274, 37111-37116 (1999).
- [5]. Merényi G., Lind J., Engman L.: J. Phys. Chem., 100, 8875-8881 (1996).
- [6]. Engman L., Lind J., Merényi G.: J. Phys. Chem., 98, 3174-3182 (1994).
- [7]. Huie R.E., Clifton C.L., Neta P.: Radiat. Phys. Chem., 92, 477 (1991).
- [8]. Sanaullah, Wilson S., Glass R.S.: J. Inorg. Biochem., 55, 87-99 (1994).
- [9]. Schöneich Ch.: Arch. Biochem. Biophys., 397, 370-376 (2002).
- [10]. Edsall J.T., Falsenfeld G., Goodman D.S., Guard F.R.N.: J. Am. Chem. Soc., 76, 3054-3061 (1954).
- [11]. Li N.C., White J.M., Dood E.: J. Am. Chem. Soc., 76, 6219-6223 (1954).

POLY(SILOXANEURETHANES) AS SCAFFOLDS FOR TISSUE ENGINEERING

Izabella Legocka, Monika Celuch, Jarosław Sadło

Sterilization process using the radiation method may be connected with some structural changes of the polymer material. So, the optimization of sterilization process parameters and at the same time optimization of chemical structures of polymer materials selected to meet specific requirements for biomedical applications are very important.

The main scope of the presented study is to observe and understand the influence of sterilization process by the radiation method on chemical and structural changes of experimental segmented poly(siloxaneurethanes) (PSU) designed for medical scaffolds for tissue engineering.

It is known that under irradiation conditions free radicals in polymers are formed. Kinetics of initiation and decaying of these radicals as a function of structure of segmented PSU was investigated.

One of the area of our interest are polymers designed for tissue engineering as scaffold tissue. Such polymers should meet basic requirements:

- to make it possible cells adherence to scaffold surface, that means that there should be achieved optimal hydrophobic-hydrophilic surface balance;
 - to make it possible growing new cells, so no toxic substances should be produced;
 - to have adequate mechanical properties.
- All the above parameters of polymeric scaffolds should be held after radiation sterilization.
- Very interesting polymers owing to their useful properties are polyurethanes and segmented PSU. They have a chemical structure which can be modified in a very large range. The mentioned polymers are characterized by:
- very good mechanical properties;
 - possibility of frothing which indicates that their macrostructure is useful for mechanical cells settling;
 - good chemical resistance;
 - surface structure which can be relatively easy modified.

Table 1. Chemical composition of selected PSU.

Number of sample	Chemical structure of samples			
	NCO/OH ratio	oligosiloxanediol		
1519	2:1	$\text{HO-R} \left[\begin{array}{c} \text{Me} \\ \\ \text{Si-O} \\ \\ \text{Me} \end{array} \right]_n \left[\begin{array}{c} \text{Me} \\ \\ \text{Si-R-OH} \\ \\ \text{Me} \end{array} \right]$	n=30	R = $-(\text{CH}_2)_6-$
1515	3.5:1		n=30	R = $-(\text{CH}_2)_6-$
1461	2:1		n=40	R = $-(\text{CH}_2)_3-\text{O}-(\text{CH}_2)_2-$
1463	3.5:1		n=40	R = $-(\text{CH}_2)_3-\text{O}-(\text{CH}_2)_2-$
1518	2:1		n=10	R = $-(\text{CH}_2)_6-$
1522	3.5:1		n=10	R = $-(\text{CH}_2)_6-$
1456	3.5:1		n=20	R = $-(\text{CH}_2)_3-\text{O}-(\text{CH}_2)_2-$